ЖУРНАЛ СТРУКТУРНОЙ ХИМИИ

2017. Том 58, № 2 *Февраль – март* *С. 321 – 331*

UDC 541.6:547.12

STRONG HYDROGEN BONDED SUPRAMOLECULAR ARCHITECTURE IN A CRYSTAL OF THE {3-[2-(1,3-BENZODIOXOL-5-YL)-7-METHOXY-1-BENZOFURAN-5-YL] PROPYL} DIETHYLAMINE CATION WITH THE HYDROGEN BONDED CHLORIDE HYDRATE ANION (HALIDES) ASSEMBLY: X-RAY STRUCTURE, DFT CALCULATIONS, HIRSHFELD SURFACE ANALYSIS

G. Yakalı[1], S.E. Öztürk[2], M. Aygün[3]

[1]*Department of Opticianry, Vocational School of Higher Education, Akdeniz University, Antalya, Turkey*
E-mail: gulyakali@akdeniz.edu.tr
[2]*Department of Chemistry, Faculty of Sciences, Ege University, İzmir, Turkey*
[3]*Department of Physics, Faculty of Sciences, Dokuz Eylül University, İzmir Turkey*

Received November, 8, 2015

A hydrogen bonded chloride hydrate assembly $\{[(H_2O)Cl]\}^{-\infty}$ is ion-countered by organic molecular $[C_{23}H_{28}NO_4]^+$ cations and the crystal structure of {3-[2-(1,3-benzodioxol-5-yl)-7-methoxy-1-benzofuran-5-yl] propyl} diethylamine $[C_{23}H_{28}NO_4]^+ \cdot [H_2OCl]^-$ is synthesized. Its structure is studied using X-ray crystallography. The molecular geometrical parameters, frontier molecular orbital energies (HOMO, LUMO), their energy gap (ΔE), molecular electrostatic potential analysis of the compound are calculated by DFT/B3LYP at the 6-311G(*d*,*p*) level. Benzofuran and benzodioxo ring systems of the title compound, except the diethylamine group, are essentially planar and a dihedral angle between the ring systems is 7.38(14)°. The complex compound crystallizes in the monoclinic space group $P21/c$, with $a = 15.230(4)$ Å, $b = 11.418(2)$ Å, $c = 12.880(3)$ Å, $\beta = 94.56(3)°$, $V = 2232.8(9)$ Å^3, $D_{calc} = 1.297$g/cm^3, $Z = 4$. The hydrogen bonded chloride hydrate is self-assembled to form a supramolecular array of strong N—H…Cl and O—H…Cl bifurcated hydrogen bonds making tetramers which consist of a fused four-membered ring with a graph-set descriptor and a pseudo cyclic centrosymmetric $R_2^2(8)$ ring motif. The hybrid dihalide-dihydrate clusters of $[Cl_2(H_2O)_2]^-$ are observed in the compound, too. The supramolecular crystal packing is consolidated by these bifurcated hydrogen bonds and the stacking of the sheet through strong π…π interactions. Moreover, the chain hydrogen bonds form intermolecular and intramolecular C—H…O hydrogen bonds and the 1D supramolecular array is organized by C—H…π interactions. The intercontacts in the crystal structure are analyzed using the Hirshfeld surfaces computational method. The calculated geometrical parameters are in good agreement with the observed single crystal XRD data.

DOI: 10.15372/JSC20170212

K e y w o r d s: crystal structure, benzofuran, bifurcated hydrogen bond, chloride hydrate, supramolecular architecture, tetramers, halides, DFT, Hirshfeld surface analysis.

INTRODUCTION

Benzofuran is considered as an important class of heterocyclic compounds [1] consisting of fused benzene and furan rings [2]. It is the ″parent″ of many related compounds with more complex structures and is present in numerous bioactive natural products as well as pharmaceuticals and

polymers. In this study, the ongoing studied structure is a benzofuran derivative derived from egonol scaffold which is reported previously [3, 4].

Solvated halides, particularly the chloride hydrates, are of immense importance in a variety of processes due to their ubiquity in nature; consequently, they continue to be extensively studied [5—7]. Areas of interest include, for example, aqueous salt interfaces, biologically important water/membrane interfaces, electrical phenomena in the troposphere and ionosphere, and the mobility of ions. It has been found that chloride anions in monochloride hydrates are invariably located at the surface of the water clusters, and so these clusters all have low energy polar structures [8—12]. Chloride hydrate structures are almost invariably a part of a hydrogen bonding network. An increase in the concentration has a detrimental effect on the natural hydrogen bonded network of water molecules. In the presence of halide ions solvent molecules can form various types of supramolecular synthons in crystal lattices, such as solvent (e.g. water or methanol) clusters and hybrid halogen solvent clusters. They can produce different supramolecular architectures, such as chains, rings, tapes, layers or cubes, which have attracted the interest of many research groups [13].

The functional self-assembly of molecular frameworks has attracted intense interest due to the intricate structural topologies in *Nature*. The foundation of the programmed self-assembly is built upon a detailed understanding of the way in which weak interactions participate in a reversible and self-correcting cooperative process that can respond to changes in environmental conditions, including solvent, pH, temperature, concentration, etc. [14, 15]. Self-assembly can often lead to host complexes that are very efficient for uptake and release of guests under controlled conditions [14—16]. One-dimensional chains and tapes of water clusters are notably stabilized in the templates of metal-organic supramolecular channels [17].

Crystallographic studies provide a useful probe for investigating the supramolecular architecture of such complexes. In a continuation of our interest regarding the structural characterization of these important organic complexes and their supramolecular arrangements, we now report the X-ray analysis, Hirshfeld surface analysis of DFT calculations of {3-[2-(1,3-benzodioxol-5-yl)-7-methoxy-1-benzofuran-5-yl] propyl} diethylamine chloride-hydrate $C_{23}H_{28}NO_4^- \cdot ClH_2O^+$. It was performed in order to determine its inherent conformation and describe the crucial role of hydrogen bonds to water and chloride ions and intermolecular-intramolecular interactions in the assembly of its supramolecular network. Hydrogen bonds to water and chloride ions in this study are known as bifurcated H bonds and may describe an instance at which two H-bond donors are bound to a single acceptor [10]. This three-centered (bifurcated) hydrogen bonding has been used to explain a large number of biological structures and is commonly used by biochemists and biologists to account for certain interactions in biological systems [18, 19].

EXPERIMENTAL AND COMPUTATIONAL METHODS

The synthesis of the compound is reported as ″Synthesis of egonol derivatives and their antimicrobial activities″ by S.E. Öztürk et al., 2011 and as ″Synthesis and antibacterial activity of egonol derivatives″ by S.E. Öztürk et al., 2008 [3, 4].

A good quality single crystal specimen with dimensions of 0.2662×0.2302×0.1011, whose emperical formula is $C_{23}H_{30}ClNO_5$ and the formula weight is 435.93, was selected for the X-ray diffraction experiment at $T = 293(2)$ K. It was mounted with epoxy glue at the tip of glass capillaries. The complex compound crystallizes in the monoclinic space group $P21/c$, with $a = 15.230(4)$ Å, $b = 11.418(2)$ Å, $c = 12.880(3)$ Å, $\beta = 94.56(3)°$, $V = 2232.8(9)$ Å^3, $D_{calc} = 1.297$ g/cm^3, $Z = 4$, $F(000) = 928.0$ and h range of $-17 \rightarrow 20$, k range of $-8 \rightarrow 15$, l range of $-16 \rightarrow 16$. Diffraction data were collected on an Oxford Diffraction X-Calibur equipped with an Eos-CCD detector, operated at 50 kV and 40 mA with graphite monochromated MoK_α ($\lambda = 0.71073$ Å) radiation in φ and scan modes in the range of $3.17° < \theta < 9.04°$ for the compound. The absorption corrections of the collected data for the compound was made using the CrysAlisPro program [20] and the absorption coefficient is determined as 0.205 mm^{-1}. Extinction correction was not applied. Using Olex2 [21], the structure was solved with the SHELXS structure solution program using the Direct Methods and refined with the SHELXL

using least squares minimization; completeness θ_{max} = 99.99 % on the positionaland anisotropic temperature parameters of the nonhydrogen atoms, or equivalently corresponding to 286 crystallographic parameters [22]. The positions of hydrogen atoms on their respective parent carbon atoms were generated geometrically C—H = 0.96 Å and U_{iso}(H) = 1.5U_{eq}(C) for methyl H atoms, C—H = 0.97 Å and U_{iso}(H) = 1.2U_{eq}(C) for methylene H atoms, C—H = 0.93 Å and U_{iso}(H) = 1.2U_{eq}(C) for aromatic H atoms and assigned isotropic displacement parameters before the final cycle of the least squares refinement. The water molecules were also refined anisotropically and the corresponding oxygen atoms were treated with hydrogen atoms (H1WA, H1WB) found from subsequent difference Fourier electronic density maps. The final full matrix least squares refinement [$I > 2\sigma(I)$] determined R = 0.0650 and wR = 0.1068 for observed 4954 reflections. R indices for all 4954 reflections are R = 0.2128 and wR = 0.1521. The goodness-of-fit (GOOF) value is determined as 0.880. In the difference Fourier map of the compound the maximum and minimum electron densities of 0.29 and –0.19 e/Å^3, respectively, were observed. CCDC-1471360 contains the supplementary crystallographic data for this compound. These data can be obtained free of charge from the Cambridge Crystallographic Data Center *via* www.ccdc.cam.ac.uk/data_request/cif.

The calculation of the title compound was performed using the GaussView molecular visualized program and the Gaussian 09W package [23]. The molecular structure of the compound in the ground state was optimized by density functional theory (DFT) using a B3LYP hybrid functional (Becke′s three parameter hybrid functional with the Lee—Young—Parr (LYP) correlation functional) and the 6-311G(*d*,*p*) double-zeta basis set [23, 24]. The geometrical parameters (bond length, bond angle, and dihedral angle), frontier molecular orbital energies (E_{HOMO}, E_{LUMO}), molecular electrostatic potential (MEP) were obtained from the optimized structures. These results were compared with the X-ray structural parameters.

Hirshfeld surface analysis is a rather useful technique to show intermolecular contacts in a crystal structure. Hirshfeld surfaces are based on the ratio representing a weight function between the electron distribution of a sum of spherical atoms for a molecule (the promolecule) and the same sum for the whole crystal (the procrystal) [25]. It is essential to determine a normalized contact distance, given by Eq.(1), in terms of d_e, d_i and the van der Waals radii of the atoms to avoid desiderata in treatment of close contacts between large atoms. If the intermolecular contacts are shorter than the sum of van der Waals radii of the related atoms, d_{norm} is negative and these contacts are highlighted in red on the d_{norm} surface. Longer contacts are blue (d_{norm} is positive), and contacts around the sum of van der Waals radii are white on the d_{norm} surface [26].

$$d_{norm} = \frac{d_i - r_i^{vdw}}{r_i^{vdw}} - \frac{d_e - r_e^{vdw}}{r_e^{vdw}}. \quad (1)$$

It is also useful to consider the three-dimensional (3D) Hirshfeld surface with a two-dimensional (2D) fingerprint plot to define diverse types of intermolecular contacts separately [26]. The Hirshfeld surfaces and the associated 2D fingerprint plots for the title compound were calculated using CrystalExplorer 3.0 [27].

RESULTS AND DISCUSSION

In the crystal structure of the complex compound, one crystallographically independent water molecule (O1W) and chloride ion (Cl1) are observed. The crystal structure of the compound consists of discrete, well separated $[C_{23}H_{28}NO_4]^+$ organic molecular cations and one chloride anion associated with one independent water molecule. The ORTEP drawing of the structure of the hydrogen bonded chloride hydrate assembly $[(H_2O)Cl]^-$ is formed *via* N1—H1…Cl1 and O1W—H1WA…Cl1 intramolecular hydrogen bonds, which is ion-countered by the organic molecular $[C_{23}H_{28}NO_4]^+$ cations, as shown in Fig. 1.

The X-ray crystallographic analysis revealed the presence of considerably strong intramolecular and intermolecular hydrogen bonds (Fig. 2) and strong π…π and C—H…π interactions in the crystal structure (Table 1). A part of these strong hydrogen bonds and interactions is responsible for the self-assembly supramolecular architecture and packing diagram.

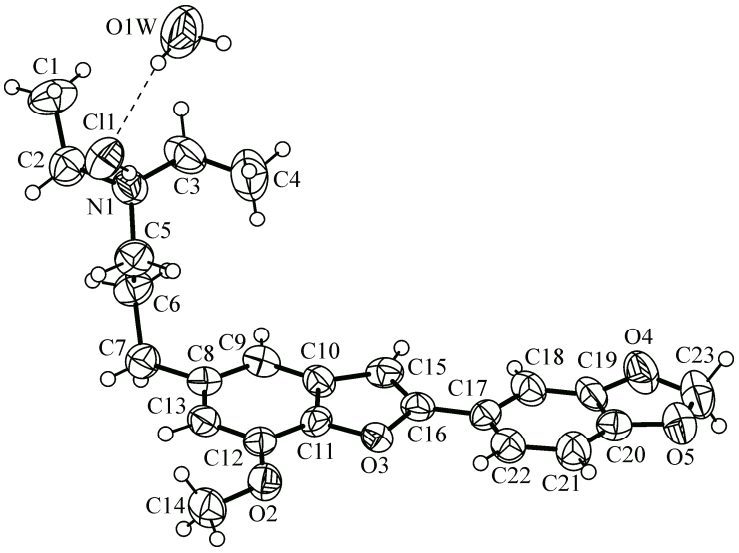

Fig. 1. Molecular geometry and atomic labeling scheme of the hydrogen bonded chloride hydrate assembly $[(H_2O)Cl]^-$ ion-countered by organic molecular $[C_{23}H_{28}NO_4]^+$ cations. Displacement ellipsoids are drawn at the 50% probability level. Dashed lines represent hydrogen bonds

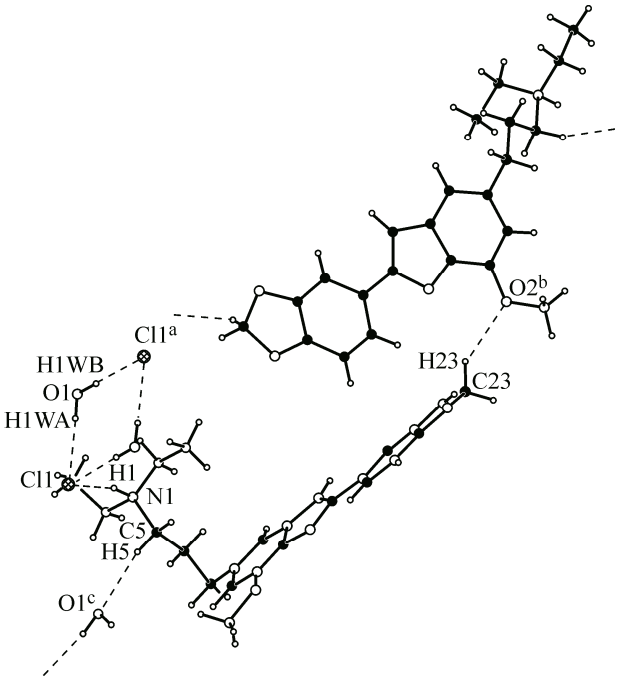

Fig. 2. N—H…Cl, O—H…Cl, C—H…O intramolecular and intermolecular strong hydrogen bonds in the crystal structure

Owing to the crystal symetry, two water molecules and two chloride ions are self-assembled due to the strong intramolecular N1—H1…Cl1, O1W—H1WA…Cl1 bifurcated hydrogen bonding [10] and the strong intermolecular O1W—H1WB…Cl1 hydrogen bonding fused over four-membered rings running along the [101] direction (Fig. 2).

These hydrogen bonding forms tetramer structures (hybrid dihalide-dihydrate clusters $[X_2(H_2O)_2]^{-2}$, X = Cl) (Fig. 4) [28]. Also, in the crystal structure, the dimeric arrangement of molecules is observed, consisting of two water molecules and two chloride ions, which form an inversion center *via* these hydrogen bonds and intermolecular strong C5—H5…O1W hydrogen bonds along the 101 plane and the four-membered ring generating the pseudo cyclic motif $R_2^2(8)$ in the Bernstein′s graph notation [29] (Fig. 3).

It is clear that the hydrogen atom of H_2O is directed towards the Cl atom. The N—H…Cl and O—H…Cl angles are 164(4)° and 174(4)°, respectively (the O—H…Cl = 172.1(2)° angle was reported by J. Dai et al., 2007 [30]). In the four membered ring the O—Cl—O angles are 77.6(2)°,

Table 1

Selected bond lengths (Å) *and angles* (deg.) *for the compound*

Bond lengths	X-ray	DFT	Bond lengths	X-ray	DFT
O2—C12	1.363(5)	1.355(2)	O5—C20	1.379(5)	1.370(2)
O2—C14	1.421(4)	1.431(2)	O5—C23	1.424(5)	1.436(2)
O3—C11	1.386(4)	1.365(2)	N1—C2	1.500(5)	1.508(2)
O3—C16	1.396(5)	1.380(2)	N1—C3	1.502(5)	1.506(2)
O4—C19	1.384(5)	1.374(2)	N1—C5	1.509(6)	1.507(2)
O4—C23	1.428(5)	1.437(2)			
Bond angles	X-ray	DFT	Torsion angles	X-ray	DFT
C12—O2—C14	117.3(3)	118.365(2)	N1—C5—C6—C7	175.7(3)	–66.850(2)
C19—O4—C23	104.0(4)	106.361(2)	C2—N1—C3—C4	–179.8(4)	–66.603(2)
C2—N1—C3	111.8(4)	112.438(2)	C2—N1—C5—C6	64.4(5)	160.906(2)
O2—C12—C11	117.1(4)	117.312(2)	C3—N1—C2—C1	–68.3(6)	–176.198(2)
O3—C16—C17	115.9(4)	116.243(2)	C3—N1—C5—C6	–62.5(5)	–179.645(2)
O4—C18—C19	126.7(5)	128.073(2)	C5—N1—C2—C1	163.4(4)	
O5—C20—C21	128.4(5)	128.634(2)	C23—O4—C19—C18	–176.3(5)	
N1—C5—C6	113.9(4)	115.758(29)	C17—C18—C19—O4	179.7(4)	

while the Cl—O—Cl angles are 102.4(2)°. Thus, the ring has a nearly tetrameric cluster. Hydrogen bonding motifs of 2D supramolecular systems have been reported as tetramers, squares, rectangles, triangles, etc. [31]. In the molecule, the average O…Cl distance of 3.2(2) Å falls in the range for hydrogen bonds between water and chloride anions [32]. (This value was reported as 3.01 Å [33]). The NCl distance is 3.113 Å (this value was reported as 3.236(2) Å [28]).

The strong intramolecular N1—H1..Cl1, O1—H1WA…Cl1 bifurcated hydrogen bonds and strong intermolecular O1W—H1WB…Cl1 hydrogen bonds and π…π interactions [Cg1…Cg4^{f} = = 3.931 Å, where Cg1 are the centroids of the furan ring (O3/C10/C11/C15/C16) and Cg4 are the centroids of the mesityl ring (C17—C22) (symetry codes: (f) *x*, 1/2–*y*, –1/2+*z*, Cg2…Cg3 =

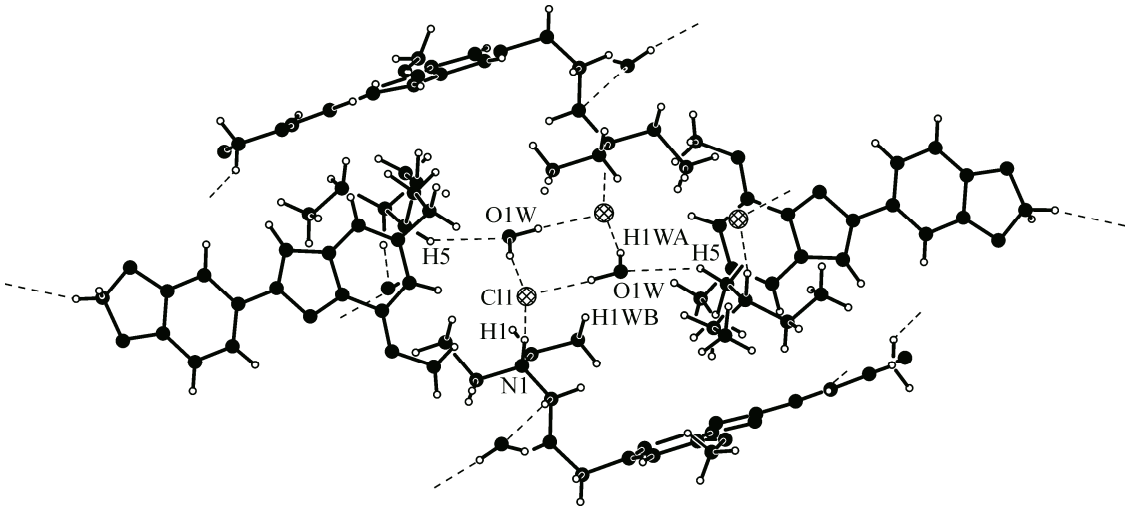

Fig. 3. The centrosymmetric hydrogen-bonded dimer structure formed by intermolecular C5—H5…O1W, O1W—H1WB…Cl hydrogen bonds and intramolecular N—H…Cl, O1W—H1WA…Cl bonds for the compound around its inversion center

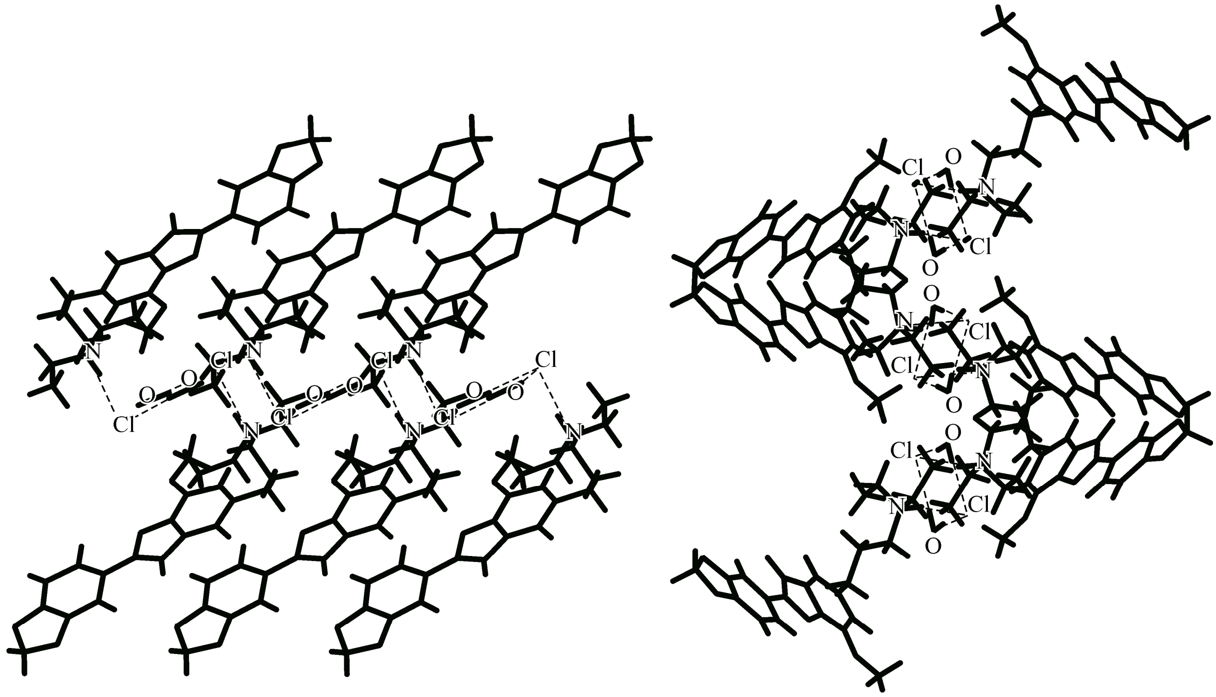

Fig. 4. Tetrameric structure of the complex in the *a*, *c*, planes of the crystal structure, respectively

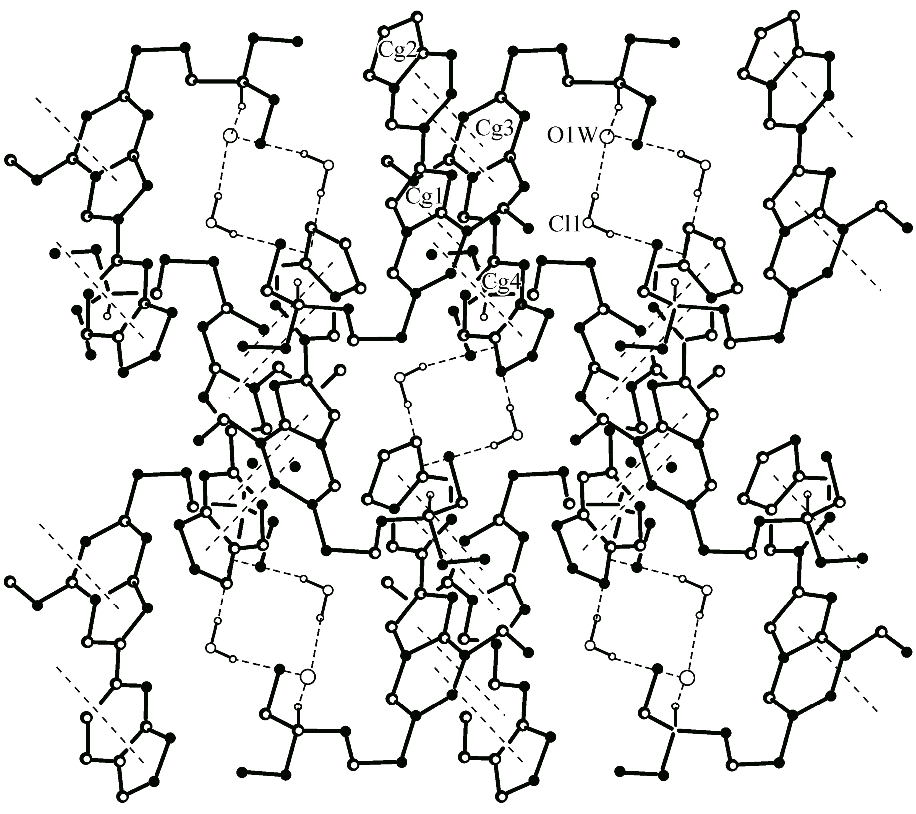

Fig. 5. Formation of the 2D supramolecular structure of the crystal showing π…π interactions and hydrogen bonds. H bonds are omitted

= 3.857(3) Å), where Cg2 are the centroids of the benzoxo ring (O4/O5/C19/C20/C23) and Cg3 are the centroids of the mesityl ring (C8—C13) are responsible for the crystal packing (Fig. 5).

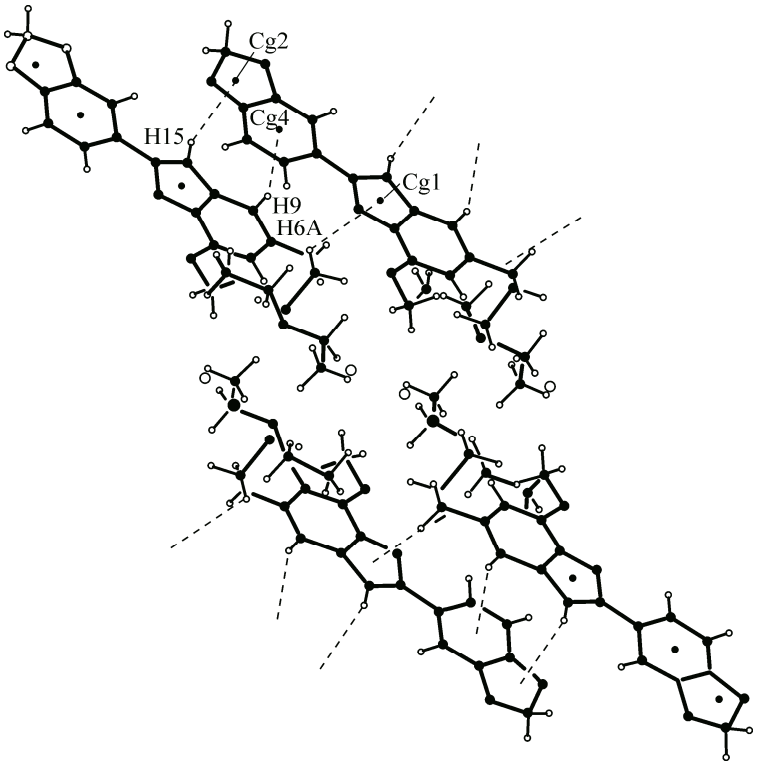

Fig. 6. 1D supramolecular array formed by C—H…π interactions in the crystal structure along the (010) plane

The two-dimensional supramolecular array of the studied complex can be analyzed in terms of various components such as centrosimetric dimer motifs, chains, and π—π interactions (Fig. 4) between the aromatic rings leading to a further stabilization of the crystal structure. Also the 1D supramolecular array is organized by C—H…π interactions (Fig. 6).

The molecule is essentially planar except for the propyl diethylamine substutient at C8 with a C6—C7—C8—C9 torsion angle of –58.1(6)°. The benzofuran ring system (C8—C16, O3) and the benzodioxo ring system (C17—C23, O4, O5) of the compound are essentially planar with a maximum deviation from the plane of 0.056(6) Å for C23, –0.012(4) Å for C10 respectively, and the dihedral angle between the ring systems is 7.38(14)°. Generally, the bond lenghts and bond angles of the ring system are normal [31, 32]. Selected bond lengths and angles of the molecule are given in Table 2.

T a b l e 2

Hydrogen bond geometry (Å, deg.) *for the compound*

Bond	D—H, Å	H…A, Å	D…A, Å	D—H…A, deg.
N1—H1…Cl1	1.02(5)	2.12(5)	3.113(5)	164(4)
O1W—H1WB…Cl1[a]	0.93(5)	2.24(5)	3.17(7)	174(5)
O1W—H1WA…Cl1	0.81(7)	2.45(7)	3.238(6)	167(7)
C23—H23…O2[b]	0.97	2.46	3.296(6)	145
C22—H22…O3	0.93	2.49	2.819(6)	101
C5—H5A…O1[c]	0.97	2.47	3.331(8)	148
C6—H6A…Cg1[d]	0.97	2.96	3.473(5)	114
C9—H9…Cg4[d]	0.93	2.93	3.770(5)	152
C15—H15…Cg2[d]	0.93	2.93	3.727(5)	145

Symetry codes: [a] 1–*x*, 1–*y*, 1–*z*, [b] 2–*x*, –1/2+*y*, 1/2–*z*, [c] 1–*x*, 1/2+*y*, 3/2–*z*, [d] *x*, 3/2–*y*, 1/2+*z*.

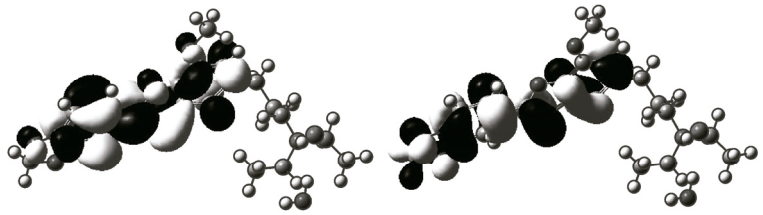

HOMO (E_{HOMO} = –4.192 eV) LUMO (E_{LUMO} = –1.438 eV)

Fig. 7. Frontier molecular orbital surfaces and energy levels for the HOMO and LUMO of the compound

In order to investigate its stability, the obtained optimized geometrical parameters were summarized in Table 2 and compared with the XRD data for the compound.

The calculation gives structural parameters that are significantly closer to those found in our X-ray study. The O…Cl distance is calculated as 3.182(2) Å and the N…Cl distance is calculated as 3.01 Å, which agree with the X-ray values obtained by the calculation. Similarly, the angles are in excellent agreement: N—H…Cl and O—H…Cl are measured as 165.11(2)° and 171.60(2)° respectively. Other geometrical parameters are coherent with X-ray values.

The highest occupied molecular orbital (HOMO) and the lowest unoccupied molecular orbital (LUMO) are the main orbitals that take part in chemical stability. The HOMO represents the ability to donate an electron, LUMO as an electron acceptor represents the ability to obtain an electron (Fig. 7). This also predicted that the nature of electrophiles and nucleophiles to the atom where the HOMO and LUMO are stronger [34].

In this title compound, the highest electronic energy exhibited at 116th is calculated as about –5.63 eV. The lowest electronic energy exhibited at the 117th virtual orbital is measured as a LUMO value of –1.438 eV. The HOMO-LUMO energy gap is determined to be about –4.192 eV, which makes the molecule more stabile and less reactive. The total energy (E_{total}) and the dipole moment of the molecule are calculated as –1785.947 Hartree and 10.0819 D, respectively. The HOMO electron density is located on the benzodioxo ring whereas in LUMO it is mostly located on the fused benzofuran ring.

The chemical hardness is 2.096 eV, which is approximated using the equation $\eta = (E_{LUMO} - E_{HOMO})/2$; the electronegativity is 3.534 eV, which is determined using the equation $\chi = -(E_{HOMO} + E_{LUMO})/2$; the electronic chemical potential is –2.096, which is determined using the equation $\mu = (E_{HOMO} + E_{LUMO})/2$; and the global electrophilicity index (ω), introduced by Parr, is –3.534 eV, which is calculated using the electronic chemical potential and the chemical hardness as shown in the equation $\omega = \mu^2/2\eta$. They were calculated using DFT [35].

The molecular electrostatic potential (MEP) is very useful as a reactivity map displaying a probable region for the electrophilic attack, the nucleophilic reaction, and the hydrogen bonding interaction of organic molecules. In order to predict the reactive site of the electrophilic and nucleophilic attacks of the title compound, MEP was also calculated with the B3LYP/6-311G(*d*,*p*) optimized geometry. The negative region of MEP (*A* region), which is around the oxygen and Cl atoms, was related to the electrophilic reactivity, and the positive region (*B* region), which is around the hydrogen atoms, corresponds to the nucleophilic reactivity (Fig. 8).

The 2D fingerprint plots of various intermolecular interactions obtained from the Hirshfeld surface of the compound are given in Fig. 9. 2D fingerprint plots of the Hirshfeld surface are of significance in determining the intermolecular interactions of crystallographically obtained molecular geometries. The chart indicates that the contribution of intercontacts to the Hirshfeld surfaces is: H…H (50.5 %), Cl…H (8.9 %), O…H (22.3 %), O…H,

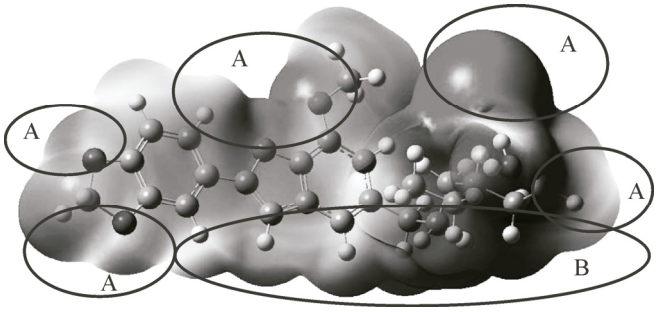

Fig. 8. Molecular electrostatic potential diagram of the title compound (*A* — negative region; *B* — positive region)

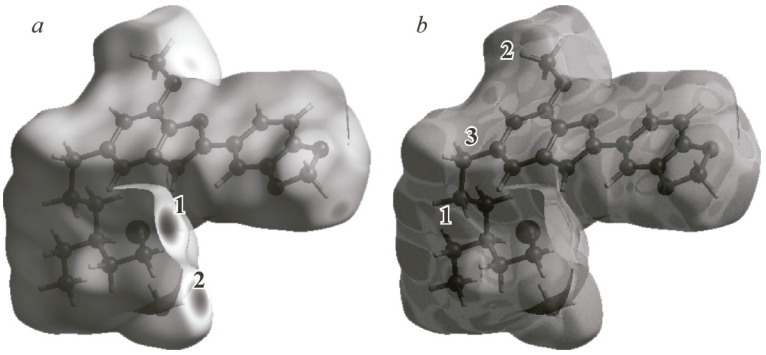

Fig. 9. Hirshfeld surface mapped with d_{norm} (*a*) and the shape index (*b*) for the compound. The surface is partially transparent for clarity

H…C (indicate C—H…π) (12 %). These intermolecular interactions are highlighted by the conventional mapping of d_{norm} on the molecular Hirshfeld surfaces (Fig. 9). In d_{norm} the black pointed spots (1, 2, and 3) show the O1W—H1WB…Cl1, C5—H5…O1, and C23—H23…O2 intermolecular interactions.

The fingerprint plot at $d_e \approx d_i < 1.2$ Å (van der Waals radius of the H atom); the hydrogen bonds characteristically evidence themselves as spikes [36]. H…H intercontacts (Fig. 10, *a*) show large surfaces. H…C/C…H also known as C—H…π interactions appear as a pair of ″wings″ in Fig. 10, *d*. C…H…π and the π-ring interaction reveal themselves also on the Hirshfeld surface mapped with a concave surface (1, 2, and 3 regions) with the shape index (Fig. 9, *b*) [36]. H…O/O…H interactions (Fig. 9, *c*) appear as distinct spikes in the fingerprint plot. H…Cl/Cl…H interactions are responsible for the O—H…Cl hydrogen bond in the crystal structure.

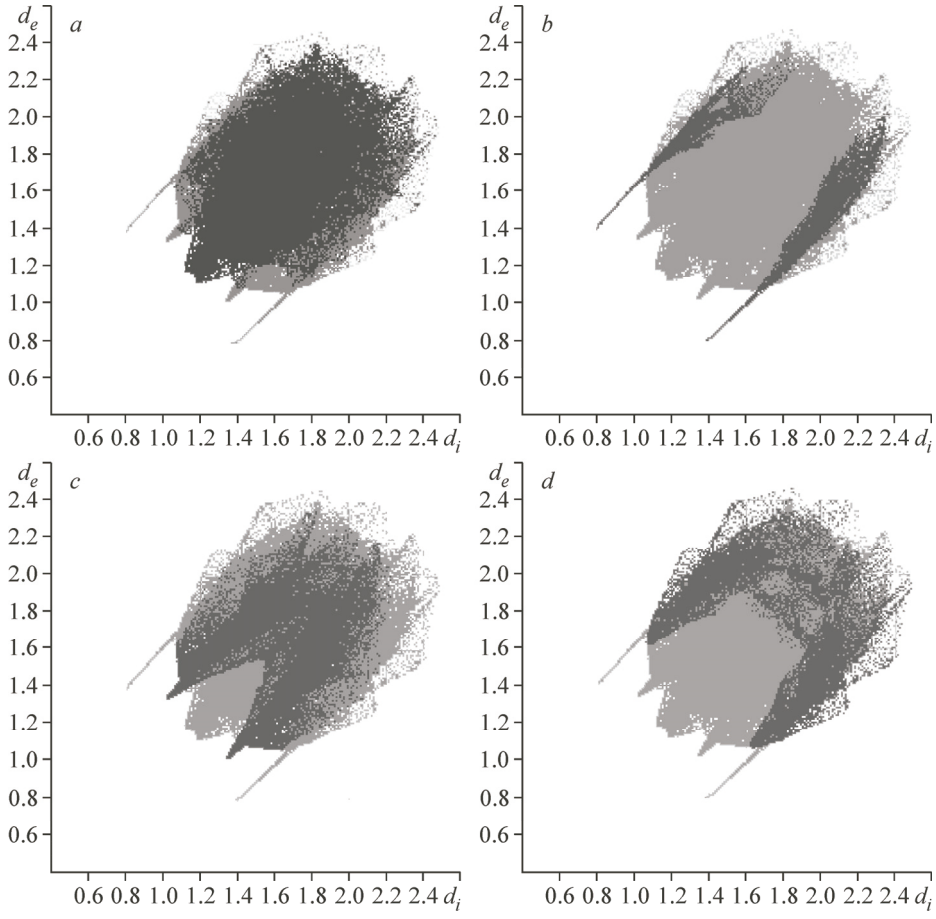

Fig. 10. Fingerprint plots of the compound: H…H contacts (*a*), reciprocal H…O/=…H contacts (*b*), reciprocal H…S/S…H contacts (*c*), reciprocal H…C/C…H contacts (*d*), mainly indicating the C—H…π interactions

CONCLUSIONS

In this study, the X-ray structural analysis revealed that the crystal structure of the compound consisted of discrete, well separated organic molecular $[C_{23}H_{28}NO_4]^+$ cations and one chloride anion associated with one independent water molecule. The chloride anion and the water molecule are bonded to the organic molecular cation *via* bifurcated hydrogen bonds. The strong intramoleculer and intermolecular hydrogen bonds and strong π…π, C—H…π interactions are observed in the crystal structure. The crystal structure is stabilizated *via* these hydrogen bonds, and these interactions and 2D and 1D supramolecular arrays can be analyzed in terms of various components, such as centrosimetric dimer motifs, chains with hydrogen bonds, and π—π interactions. The intercontacts in the crystal structure are analyzed using the Hirshfeld surface computational method. The tetrameric structure and halide clusters are observed in the crystal structure. Theoretical calculations are found to be in good agreement with the experimental XRD structural parameters.

This work has been completed at Dokuz Eylül University and is the subject of the forthcoming Ph.D. Thesis of Gül Yakalı. The authors acknowledge Dokuz Eylül University for the use of the Agilent Xcalibur Eos diffractometer (purchased under University Research Grant No: 2010.KB.FEN.13).

REFERENCES

1. *Nevagi R.J., Dighe S.N., Dighe S.N.* // Eur. J. Med. Chem. – 2015. – **97**. – P. 561 – 581.
2. *Khanam H., Shamsuzzaman* // Eur. J. Med. Chem. – 2015. – **97**. – P. 483 – 504.
3. *Öztürk S.E., Akgül Y., Anıl H.* // ScienceDirect. – 2008. – **16**. – P. 4431 – 4437.
4. *Öztürk S.E., Karayıldırım T., Anıl H.* // Bioorg. Med. Chem. – 2011. – **19**. – P. 1179 – 1188.
5. *Marcus Y*. Ion Solvation. – Chichester: Wiley, 1986.
6. *Richens D.T*. The Chemistry of Aqua Ions, Chichester: Wiley, 1997.
7. *Ohtaki H., Radnai T.* // Chem. Rev. – 1993. – **93**. – P. 1157.
8. *Lakshminarayanan P.S., Suresh E., Ghosh P.* // Angew. Chem., Int. Ed. – 2006. – **45**. – P. 3807.
9. *Custelcean R., Gorbunova M.G.* // J. Am. Chem. Soc. – 2005. – **127**. – P. 16362.
10. *Kemp D.D., Gordon M.S.* // J. Phys. Chem. A. – 2005. – **109**. – P. 7688.
11. *Robertson W.H., Johnson M.A*. // Ann. Rev. Phys. Chem. – 2003. – **54**. – P. 173.
12. *Ayala R., Martínez J.M., Pappalardo R.R., Marcos E.S.* // J. Chem. Phys. – 2003. – **119**. – P. 9538.
13. *Trzybin'ski D., Sikorski A*. // CrystEngComm. – 2013. – **15**. – P. 6808 – 6818.
14. *Structure* and Bonding. Vol. 96: Molecular Self-Assembly. Organic versus Inorganic Approaches / ed. by M. Fujita. – Springer, 2000.
15. *Desiraju G.R.* Crystal Engineering: The Design of Organic Solids. – Amsterdam: Elsevier, 1989.
16. *Lehn J.-M.* Supramolecular Chemistry – Concepts and Perspectives. – Weinheim: VCH, 1995.
17. *Li F., Li T.H., Su W., Gao S.Y., Cao R.* // Eur. J. Inorg. Chem. – 2006. – P. 1582 – 1587.
18. (a) *Jeffrey G.A., Takagi S.* // Acc. Chem. Res. – 1978. – **11**. – P. 264. (b) *Jeffrey G.A., Maluszynska H.* // Int. J. Biol. Macromol. – 1982. – **4**. – P. 173. (c) *Jeffrey G.A., Mitra J.* // J. Am. Chem. Soc. – 1984. – **106**. – P. 5546.
19. *Rozas I., Alkorta I., Elguero J.* // J. Phys. Chem. – 1998. – **102**. – P. 9925 – 9932.
20. *CrysAlisPro* and CrysAlisRed. – Yarnton, Oxfordshire, England: Agilent Technologies, 2002.
21. *Dolomanov O.V., Bourhis L.J., Gildea R.J., Howard J.A.K., Puschmann H.* // J. Appl. Cryst. – 2009. – **42**. – P. 339 – 341.
22. *Sheldrick G.M.* // Acta Crystallogr. A. – 2008. – **64**. – P. 112.
23. *Frisch M.J., Trucks G.W., Schlegel H.B., Scuseria G.E., Robb M.A., Cheeseman J.R., Montgomery J.A., Vreven J.T., Kudin K.N., Burant J.C., Millam J.M., Iyengar S.S., Tomasi J., Barone V., Mennucci B., Cossi M., Scalmani G., Rega N., Petersson G.A., Nakatsuji H., Hada M., Ehara M., Toyota K., Fukuda R., Hasegawa J., Ishida M., Nakajima T., Honda Y., Kitao O., Nakai H., Klene M., Li X., Knox J.E., Hratchian H.P., Cross J.B., Adamo C., Jaramillo J., Gomperts R., Stratmann R.E., Yazyev O., Austin A.J., Cammi R., Pomelli C., Ochterski J.W., Ayala P.Y., Morokuma K., Voth G.A., Salvador P., Dannenberg J.J., Zakrzewski V.G., Dapprich S., Daniels A.D., Strain M.C., Farkas O., Malick D.K., Rabuck A.D., Raghavachari K., Foresman J.B., Ortiz J.V., Cui Q., Baboul A.G., Clifford S., Cioslowski J., Stefanov B.B., Liu G., Liashenko A., Piskorz P., Komaromi I., Martin R.L., Fox D.J., Keith T., Al-Laham M.A., Peng C.Y., Nanayakkara A.,*

Challacombe M., Gill P.M.W., Johnson B., Chen W., Wong M.W., Gonzalez C., Pople J.A. Gaussian 03, Revision E. 01. – Pittsburgh, PA: Gaussian Inc., 2003.
24. *Frisch A., Dennington R.D., Keith T.A., Milliam J., Nielsen A.B., Holder A.J., Hiscocks J*. GaussView Reference, Version 4.0. – Pittsburgh: Gaussian Inc., 2007.
25. *Spackman M.A., Jayatilaka D*. // CrystEngComm. – 2009. – **11**. – P. 19 – 32.
26. *Spackman M.A., McKinnon J.J*. // CrystEngComm. – 2002. – **4**. – P. 378 – 392.
27. *Wolff S.K., Grimwood D.J., McKinnon J.J., Turner M.J., Jayatilaka D., Spackman M.A*. CrystalExplorer (Version 3.0). – University of Western Australia, 2012.
28. *Trzybinski D., Sikorski A*. // CrystEngComm. – 2013. – **15**. – P. 6808.
29. *Etter M.C., MacDonald J.C., Bernstein J*. // Acta Crystallogr. B. – 1990. – **46**. – P. 256 – 262.
30. *McKinnon J.J., Jayatilaka D., Spackman M.A*. // Chem. Commun. – 2007. – P. 3814 – 3816.
31. *Chakrabarty R., Mukherjee P.S., Stang P.J*. // Chem. Rev. – 2011. – **111**, N 11. – P. 6810 – 6918.
32. *Dai J.X., Wu F.H., Yao W.R., Zhang Q.F*. // Z. Naturforsch. – 2007. – **62b**. – P. 491 – 494.
33. *Lundgren J., Olovsson I*. // Acta Crystallogr. – 1967. – **23**. – P. 971.
34. *Babu N.R., Subashchandrabose S., Padusha M.S.A., Saleem H., Erdoğdu Y*. // Mol. Biomol. Spectrosc. – 2014. – **120**. – P. 314 – 322.
35. *Murugavel S., Manıkandan N., Lakshmanan D., Naveen K., Perumal P.T*. // J. Chil. Chem. Soc. – 2015. – **60**. – P. 3.
36. *McKinnon J.J., Spackman M.A., Mitchell A.S*. // Acta Crystallogr. B. – 2004. – **60**. – P. 627 – 668.